Electrophoresis of model colloidal spheres in low salt aqueous suspension

2004 J. Phys.: Condens. Matter 16 S4039

(http://iopscience.iop.org/0953-8984/16/38/019)

INSTITUTE OF PHYSICS PUBLISHING JOURNAL OF PHYSICS: CONDENSED MATTER

J. Phys.: Condens. Matter **16** (2004) S4039–S4050 PII: S0953-8984(04)78992-4

Electrophoresis of model colloidal spheres in low salt aqueous suspension

Thomas Palberg[1], Martin Medebach[1], Norbert Garbow[1], Martin Evers[1], Ana Barreira Fontecha[1], Holger Reiber[1] and Eckhard Bartsch[2]

[1] Johannes Gutenberg Universität Mainz, Institut für Physik, Staudinger Weg 7, D-55128 Mainz, Germany
[2] Johannes Gutenberg Universität Mainz, Institut für Physikalische Chemie, Welder Weg 15, D-55128 Mainz, Germany

Received 13 April 2004
Published 10 September 2004
Online at stacks.iop.org/JPhysCM/16/S4039
doi:10.1088/0953-8984/16/38/019

Abstract

We report on comprehensive measurements of the electrophoretic mobility μ of a highly charged spherical colloid in deionized or low salt aqueous suspensions, where fluid and crystalline order develops with increased packing fraction Φ. We propose the existence of a 'universal' shape of the $\mu(\Phi)$ showing three distinct regimes: a logarithmic increase, a plateau and a logarithmic decrease. The position and the height of the plateau are found to be influenced by the particle surface properties and the electrolyte concentration. In particular, it starts once the counter-ion concentration becomes equal to the concentration of background electrolyte. This coincides only loosely with the range of Φ where fluid order is developing. Also the better defined first order freezing transition is observed to be uncorrelated to the shape of the $\mu(\Phi)$ curve.

1. Introduction

In many situations surfaces, particles and fluids bear electric charges. Electrokinetic effects (i.e. relative motion between these three kinds of objects) arise upon the application of external electric fields. The electrophoretic effect denoting the motion of a charged particle through an electrolyte has been known for more than a century. In an electrostatic field E the particle will acquire a stationary drift velocity $v_E = \mu E$, where the mobility μ is related to the surface or ζ-potential, which in turn corresponds to the particle charge Z [1]. While for all practical purposes, and for isolated particles, this is well captured by mean-field theories on different levels of sophistication [2], a deeper problem remains in the relation between static and dynamic properties. For example the static description of the particle fluid interface is now rather well understood, using either the mean field Poisson–Boltzmann description, or more sophisticated integral equations suited to account for correlations of ionic charges [3]. The notion of electric

double-layer and the surface potential is a central concept to understand these properties. Open questions here rather concern the effective interactions between particles (pair interactions, many body terms, effective attraction between like charged particles) and the emergence collective properties like phase behaviour or elasticity. On the other hand the concept of the ζ-potential relates to the existence and positioning of a dynamically defined plane of shear, not necessarily coincident with the particle surface. The potentially strong connections between slippage phenomena (crucially depending on hydrophobicity, surface roughness and electrostatic 'binding' of counter-ions) and electro-kinetic effects remains obscure. These complex relations between different theoretical aspects call for the combined effort of theory, simulation and experiment. We here shall provide the latter by an extended investigation of the particle concentration dependence of the electrophoretic mobility.

On the practical side, the electrophoretic effect has found wide and successful applications for characterization and preparative purposes in both technical and biological systems, where at process or physiological conditions any electrostatic interactions are sufficiently screened to stay in the isolated particle limit. Still, much less is known about electrophoresis at low salt conditions or in the deionized state. Under such circumstances the ionic atmospheres surrounding each charged particle grow very large and may overlap with neighbouring ones, leading to a strong and long-ranged screened Coulomb repulsion and the formation of fluid or even crystalline structures [4]. Only few experimental [5–11] and theoretical [12] studies have addressed electrophoresis under these conditions and up to now only for the non-interacting or fluid state. We therefore may further specify the goal of this paper to be the presentation of a solid data base for mobilities of *deionized and low salt* systems of highly charged spherical model particles over a wide range of particle concentrations.

We shall consider three separate regimes: isolated particles, development of fluid order and colloidal crystals. The challenge of measuring truly isolated particles is both in sample preparation and particle detection techniques. This has been solved by advanced conditioning procedures [13] and the development of a optical tweezing electrophoretic set-up [11], which was a consequent extension of the single particle tracking apparatus realized by Schätzel and co-workers [14, 15]. For sufficiently large particles even conventional laser Doppler velocimetry (LDV) may suffice [5], which performs excellently at elevated particle concentrations, where fluid order prevails. Heterodyne and super-heterodyne LDV under high frequency (20 Hz $< f <$ 100 Hz) ac field conditions (to avoid electro-osmotic flow) has been applied in the older literature and also here for disordered and fluid samples. It yields quite complicated spectra, difficult to evaluate quantitatively. We recently developed a super-heterodyne technique under quasi-DC conditions [16] which solved these problems and allows for a quantitative correction of the aforementioned results.

This novel technique is also applied for integral and spatially resolved measurements in the most interesting regime, the crystalline state. This state, however, has its own challenge due to the cohesion between the colloidal particles. The first order freezing transition for our crystalline samples under thoroughly deionized conditions is at a particle number density of $n = 6.2\ \mu\mathrm{m}^{-3}$. Then particle distances $d_{NN} = n^{-1/3}$ are of the order of 550 nm, i.e. eight particle diameters. At the corresponding packing fraction of 0.002 the colloidal crystal is a very porous object. Stable at room temperature, it has a small but finite shear modulus of a few pascal. It may thus be easily destroyed, i.e. shear molten, by small mechanical perturbations. In an electrophoretic experiment in a closed cell of charged walls there always exists a so-called electro-osmotic flow, i.e. a motion of ions at the cell wall, dragging along the solvent and (due to its incompressibility) a central solvent back flow. The solvent flow profile is parabolic with a high shear region close to the wall [17, 18]. This flow may strain and even shear melt the crystal or drastically slow solidification of colloidal melts [19]. For periodic fields, on the other

Table 1. Particle properties of the samples investigated. $2a$ is the nominal diameter and $2a_H$ is the hydrodynamic radius; here DLS denotes dynamic light scattering; OT the optical weezer [14] and UZ the ultra-centrifuge. N is the titrated surface group number. The Bjerrum length λ_B is different for water samples and glycerol in water solution (35% w/w). Mobilities given refer to the low salt limit for isolated particles in the water/glycerol mixture (OTE [25]). * denotes data as given by the manufacturer. # charges after extended treatment with ion exchange resin.

Sample	$2a$ (nm)	$2a_H$ (nm)	N	λ_B (nm)	μ ($\Phi = 10^{-7}$) (10^{-8} m^2 V^{-1} s^{-1})
PS306[a]	306*	301 ± 1.4 (OT)	1.67×10^5*	0.93	0.72 ± 0.05
PS301[a]	301*	322 ± 2.4 (OT)	$(2.3 \pm 0.2) \times 10^4$	0.93	0.72 ± 0.06
PS378[a]	378*	375 ± 6.8 (OT)	1.13×10^5*	0.93	0.79 ± 0.05
PS401[b]	401*	401 ± 4.5 (OT)	2.8×10^5*	0.93	0.68 ± 0.06
PS415[c]	415*	438 ± 5.0 (OT)	1.48×10^5*	0.93	0.76 ± 0.04
PS403[c]	403*	454 ± 0.9 (OT)	1.54×10^5*	0.93	0.63 ± 0.06
PS115[d]	115*	125.8 (DLS)	3.6×10^3	0.72	
PnBAPS68[e]	68 (UZ)*		11.8×10^3	0.72	
PSL2[f]	105*	102 ± 5 (DLS)	$>8 \times 10^3$; $<700^{\#}$	0.72	
PSPSS3[g]	71	70 ± 2 (DLS)*	1.2×10^4	0.72	

[a] Particles: polystyrene; surface groups: sulfate; manufacturer: Dow Chemicals, IN.
[b] Particles: polystyrene; surface groups: carboxyl; manufacturer: IDC, Portland, Oregon.
[c] Particles: polystyrene; surface groups: sulfate/carboxyl; manufacturer: IDC, Portland, Oregon.
[d] Particles: polystyrene; surface groups: sulfate; manufacturer: IDC, Portland, Oregon.
[e] Particles: poly(nbutylacrylamide/styrene) copolymer; surface groups: sulfate; manufacturer: BASF, Ludwigshafen, Germany.
[f] Particles: polystyrene; surface groups: sulfate/SDS; synthesized by A Weiss, University of Karlsruhe, Germany.
[g] Particles: poly(styrene/styrenesulfonate) copolymer; surface groups: sulfate/sulfonate; synthesized by A Weiss, University of Karlsruhe, Germany [37].

hand, mechanical vibrations of colloidal crystals may be excited [20]. In a recent series of papers we have investigated the phenomenology of electro-osmotic shear induced phenomena and pointed out similarities and differences to pure mechanical shear [21–23]. We observed a complex and fascinating flow behaviour with, e.g. plug-like flow profiles or multi-phase coexistence. Moreover we also found a complicated time dependence. In addition, we have worked out a suitable method to determine the mobility from a spatial average of the complete particle flow profile [24]. This will be employed here.

The paper is organized as follows: we first consider some important technical aspects of sample preparation and of electrophoresis measurements. We then shall present the results for salt and particle concentration dependent mobilities in different states of order. In the concluding discussion we shall address the universality of the particle concentration dependence of μ, its unresolved relation to theoretical expectations and point out a set of open questions.

2. Experimental details

2.1. Sample conditioning

In most experiments we used commercially available latex spheres. For measurements of the fluid state, in addition the samples PSL2, PSPSS3 and PnBAPS68 were used, which were kind gifts of the group of M Ballauff and the BASF, respectively. Particle were carefully characterized by various methods and a compilation of the most important data is given in table 1.

Samples of different particle number density n were prepared from pre-cleaned stock suspensions by dilution with doubly distilled water. For LDV measurements sample preparation took place in a closed, gas tight tubing system under inert gas atmosphere. The system connects several devices including a reservoir to add water or suspension, an ion exchange column filled with mixed bed ion exchange resin (Amberlite UP 604, Rohm & Haas, France), a conductivity experiment and several optical cells to simultaneously perform laser Doppler velocimetry (LDV), static light scattering and video microscopy. During preparation the suspension is driven through the circuit by a peristaltic pump. Equilibrium crystalline samples are kept in a shear molten state but readily crystallize upon cessation of shear and the measuring cell is isolated against the remaining circuit. Completion of deionization is monitored via the time dependence of the conductivity, typical residual ionic impurity concentrations are of the order of the ion product of water. The particle number density n is inferred from a combined Bragg scattering and conductivity experiment on the deionized sample [25]. Adjustment of the salt concentration c via addition of salt solution to the reservoir after complete deionization was also monitored via conductivity, using Hessinger's formula [26]. Further details of the preparation have been given elsewhere [8, 13]. We here only note that this method is fast, reproducible and accurate and in addition allows the performance of simultaneous experiments under identical conditions.

PSL2 was observed to lose most of its SDS stabilizing groups during long contact with ion exchange resin. It further became unstable against shear (pumping) induced coagulation. Its particle concentration dependence was therefore measured as provided in $10^{-3}n$ KCl solution. For measurements at no salt we performed deionization in a batch procedure (i.e. without circulation), until no further change of conductivity was observed. Charge numbers quoted in table 1 refer to charges before treatment with ion exchange resin and to the state after de-charging, with mainly sulfate groups remaining.

Also for optical tweezing electrophoresis (OTE) samples were pre-conditioned using the continuous deionization procedures. For technical reasons they then had to be filled into a batch measuring cell carefully avoiding contact with air. Sample volumes are rather small in this case and precise adjustment of c in the μmol l^{-1} range is difficult. While for individual samples c is well monitored via conductivity, the reproducibility of c for different samples is rather bad. In order to obtain the limiting values for the low salt case under equal conditions for all particle species we worked with a mixture (PS301, PS306, PS378, PS401, PS415, PS403). In addition we checked the c-dependence of μ for selected one-component samples (see below) to find no dependence of μ on c for $c < 10^{-4}$ mol l^{-1}. Therefore the uncertainty in the salt concentration of the OTE experiment on the mixture may be rather large, but the limiting low salt (deionized state) values of μ reported in table 1 are nevertheless accurate.

2.2. Electrophoresis measurements

Measurements on isolated particles were carried out using OTE with an Uzgiris type cell of square cross section with the electrodes far from the cell walls to avoid electro-osmotic flows [27]. In short, a sample of very low particle concentration is prepared and individual particles are trapped in a tube tweezer. Light pressure pushes the particle in the z-direction along the optical axis, while it is kept centred on the optical axis by gradient forces. An AC electric field of strength E and frequency ω is applied in the x-direction and the lateral elongation $A = \mu E/\omega$ is measured *via* a microscopic projection. At the same time the particle size is inferred with great accuracy from a combined analysis of drift velocity in the z-direction and intensity of back-scattered light. For further details the reader is referred to [11] and [25].

Data are collected as distributions of μ versus $2a$. Figure 1 gives an example. Limiting low salt values measured in a 35% (w/w) glycerol in water solution are compiled in table 1.

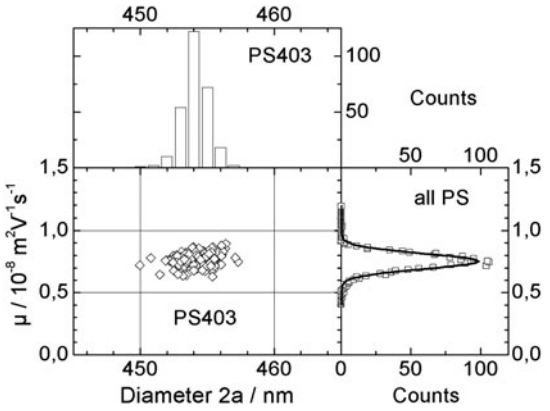

Figure 1. Mobility μ versus diameter d. Lower left panel shows a scatter-plot of all PS403 data. The top panel gives the size distribution for PS403. The right panel shows the mobility distribution for the mixture of all samples. No correlation between size and mobility is observed.

Interestingly, μ was found independent of particle size. We note that this translates to a linear dependence of electrophoretic effective charges on the particle radius, which was predicted theoretically and also observed in computer simulations [28, 29]. By comparison with data collected by LDV for water based samples, this dependence and the scaling with solvent dielectric constant were recently confirmed over an even broader size range [30].

At larger particle concentrations laser Doppler velocimetry was employed in flow-through cells of rectangular cross section with depth $\times$ height $= d \times h = 1 \times 10\ \mathrm{mm}^2$. The origin of our coordinate system is at the cell centre with $x \parallel d$, $y \parallel h$ and $z \parallel v$. For DC fields electro-osmosis leads to a parabolic flow profile for the solvent, on which the particle electrophoretic velocity is superimposed $v(x, y) = v_S(x, y) + v_E$. In an integral measurement the full x-range is observed at fixed y. The sample is illuminated by a laser beam and light scattered under an angle Θ is collected on a distant photomultiplier. A reference beam acting as a local oscillator is superimposed there to induce a beat signal with the Doppler shifted scattered light. The beat signal is FFT-analysed to yield the distribution of Doppler shifts $\omega_{\mathrm{Doppler}} = \mathbf{q} \cdot \mathbf{v}$, where $\mathbf{q}$ is the scattering vector of modulus $q = (4\pi n_S/\lambda)\sin(\Theta/2)$, where n_S is the solvent refractive index and λ is the wavelength of the laser light *in vacuo*.

Here and in previous measurements on fluid samples we used the super-heterodyning technique with AC fields of some 20–100 Hz to minimize electro-osmotic flows [8]. In contrast to conventional heterodyning, here an additional frequency shift $\Delta\omega$ is introduced between the reference beam and the illuminating beam leading to a separation of the self-beating signal and the Doppler signal by $\Delta\omega$. However, under AC conditions, the spectra showed a splitting into several peaks positioned at multiples of the AC frequency and only the envelopes could be analysed further. Data gathered this way showed a considerable statistical uncertainty.

We repeated the measurements for selected samples now employing quasi DC conditions by using square wave AC fields of 0.2–0.05 Hz and restricting the measurement intervals to one polarity, starting 1s after field reversal and ending 1s before the next [23]. This way we observed a constant additional *systematic* 20–25% difference as compared to the quasi DC heterodyne technique. We could trace that difference back to an asymmetric weighting of large velocities in the envelope evaluation procedure. All mobilities taken under high frequency AC fields and all data adapted from previous studies therefore were corrected for these errors by multiplication with 0.75.

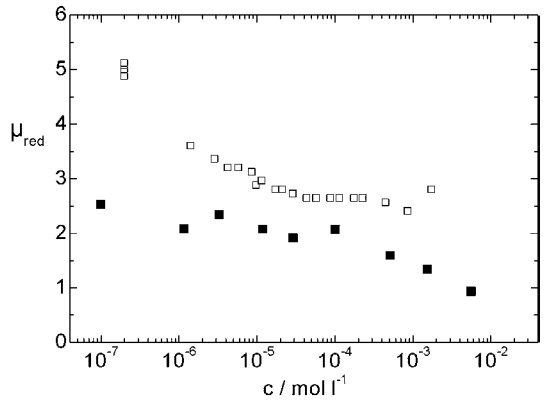

Figure 2. Reduced mobilities μ_{red} of PS301 versus salt concentration c. Filled squares: OTE at $\Phi \approx 10^{-7}$; open squares: heterodyne LDV corrected for systematic errors at $\Phi = 1.3 \times 10^{-4}$.

In the disordered and in the fluid state the flow profile is strictly parabolic and the spectra can be evaluated using well known quantitative expressions for the velocity distribution in terms of the electro-osmotic velocity of the solvent at the cell wall, the diffusivity of the particle and the electrophoretic velocity [31]. μ is there inferred from integral super-heterodyne measurements performing excellently in the disordered and the fluid state [16]. For crystalline samples we extended our technique to spatially resolved measurements by introducing some additional imaging optics into the detection path. This yielded the complete stationary flow profiles $v(x, y)$ and in addition allowed us to characterize the interesting non-equilibrium flow behaviour of colloidal crystals [21–23]. Since the solvent is incompressible the net solvent flow in any closed cell is zero and the average particle velocity may be equated to v_{E} irrespective of the structure of the suspension $\langle v(x, y)\rangle_{x,y} = v_{\mathrm{E}} = \mu E$.

3. Results

3.1. Salt concentration dependence of the electrophoretic mobility

Figure 2 shows a comparison of the salt concentration dependence of the mobility of PS301 under two different Φ and in terms of the reduced mobility

$$\mu_{\mathrm{red}} = \frac{2}{3}\frac{\eta}{\varepsilon k_{\mathrm{B}} T}\mu \tag{1}$$

where η is the solvent viscosity, $\varepsilon = \varepsilon_0\varepsilon_{\mathrm{r}}$ denotes the solvent dielectric permittivity and $k_{\mathrm{B}}T$ is the thermal energy. Note the qualitative differences between the two curves. For isolated spheres in the glycerol in water solution the mobility increases with decreasing c to level off for $c \leqslant 10^{-4}$ mol l^{-1} at values of $\mu_{\mathrm{red}} \approx 2$–2.5. At elevated concentrations the mobility first increases gradually with decreasing c but an accelerating increase is observed for $c \leqslant 10^{-5}$ mol l^{-1}. From measurements at constant Φ and under variation of solvent composition we can exclude any influences of the solvent. The different behaviour is therefore attributed to the variation in Φ. We note that similar curves have been observed before both for isolated particles [32] and at elevated particle concentration [6], but no comparison was previously given for the same species.

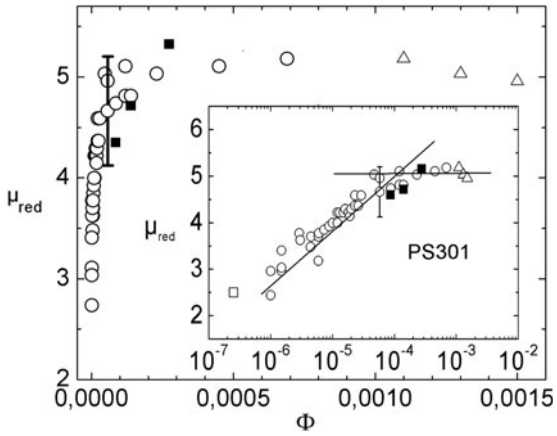

Figure 3. Reduced mobilities μ_{red} of PS301 versus decadic logarithm of the packing fraction (insert: versus packing fraction). The symbols denote different states of the suspension: □: isolated particles (OTE); ○: disordered and fluid systems (data adapted from [8] and corrected for systematic evaluation error); ●: disordered and fluid systems (data recorded using superheterodyne LDV); △: crystalline systems (data adapted from [8] and corrected for systematic evaluation error). Lines are guides to the eye.

3.2. Particle concentration dependence of the electrophoretic mobility

The lowest accessible particle number density was realized using OTE: $n = \Phi/(4\pi/3)a^3 = 1\text{–}5 \times 10^{12}$ m^{-3}. There, for all investigated particles, low reduced mobilities of 2–2.5 were observed. With increasing n the mobility rises approximately logarithmically with n, respectively, Φ. It levels off to a plateau value of 5.5 for $n > 10^{16}$ m^{-3}, respectively, $\Phi > 5 \times 10^{-5}$. For PS301 this plateau could be followed by LDV up to $n = 10^{17}$ m^{-3}, respectively, $\Phi \approx 2 \times 10^{-3}$. There the suspension becomes too turbid for further optical measurements. At $n \approx 1 \times 10^{17}$ m^{-3} a first order phase transition to the crystalline state is observed to show (within experimental error) no strong influence on μ. Open symbols in figure 3 were adapted from [8] and corrected for previous systematic evaluation errors (see above). Closed symbols show our new data.

Both the absolute value of the plateau reduced mobility and the position of the transition from the ascent to the plateau may be shifted considerably. This is shown in figures 4 and 5. In figure 4 we show $\mu(\Phi)$ for PS115 at four different salt concentrations c. With increasing c the plateau moves to lower values and its beginning shifts to larger n. Here we plotted our data versus κa, where the Debye screening parameter is defined *via*:

$$\kappa = \sqrt{\frac{e^2}{\varepsilon\varepsilon_0 k_{\mathrm{B}} T} \sum n_i z_i^2} \tag{2}$$

where e is the elementary charge, $\varepsilon\varepsilon_0$ is the dielectric permittivity of the suspension, $k_{\mathrm{B}}T$ is the thermal energy. κ^{-1} is a rule of thumb measure of the extension of the ionic atmosphere surrounding the particles. Note that the sum over the densities $n_i = 1000 N_{\mathrm{A}}\, c_i$ of all small ion species of concentration c_i and valency $z_i = 1$ not only comprises added electrolyte, and ions stemming from the self dissociation of water, but also Z^* released counter-ions per particle: $\Sigma n_i z_i = nZ^* + \Sigma 1000 N_{\mathrm{A}}\, c_i$. In the curves of figure 4 the first two terms dominate at low particle concentrations and the curves rise vertically at unchanged κ. As soon as the counter-ion term becomes significant, the curves show plateau behaviour. Obviously this way

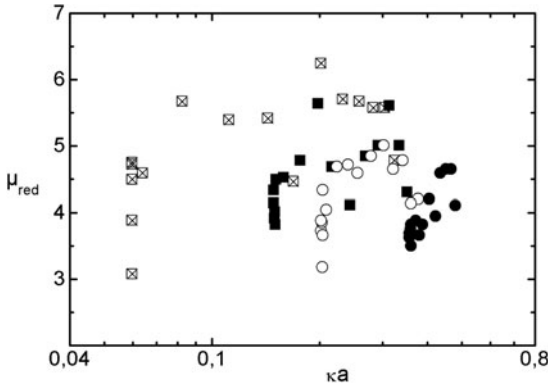

Figure 4. Reduced mobilities μ_{red} of PS115 versus κa. κa was changed at constant underlying electrolyte concentration (KCl) by increasing n measured using heterodyne LDV corrected for systematic errors. Symbols denote different c. ⊠: $c = 0$; ■: $c = 15\ \mu\mathrm{mol\,l^{-1}}$; ○: $c = 30\ \mu\mathrm{mol\,l^{-1}}$; ●: $c = 100\ \mu\mathrm{mol\,l^{-1}}$. For each data point the sample was first diluted, then it was deionized and then c adjusted under control of conductivity. Note the larger scatter of data in particular for the two moderate salt concentrations, which indicates the difficulties of meeting desired c under these conditions.

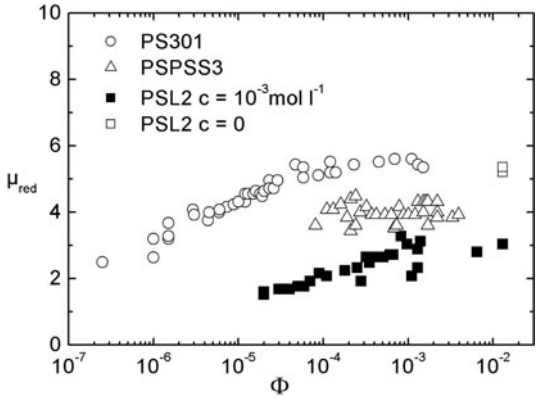

Figure 5. Reduced mobilities μ_{red} versus packing fraction for different particle species obtained from heterodyne LDV. PS301 and PSL2 in $10^{-3}n$ KCl show both a logarithmic increase and a plateau, PSPSSL3 shows a plateau only. After fast deionization μ_{red} of PSL2 had shifted to larger values. It decreased again after long deionization and particle discharging.

of plotting exaggerates the transition. Still the correspondence between the onset of the plateau and the start of counter-ions dominating the ionic strength is striking. In addition, this also coincides with the formation of fluid order. E.g. at $\kappa a = 0.83$ the height of the first peak of the static structure factor was 1.3. This correlation, however, is not pronounced due to the gradual evolution of structure with increased n.

Figure 5 shows the Φ-dependence of μ_{red} for three different species. For both smaller species samples were less turbid and μ_{red} could be measured up to larger Φ, corresponding to $n_{\mathrm{PSPSS3}} = 6.6 \times 10^{18}\ \mathrm{m^{-3}}$ and to $n_{\mathrm{PSL2}} = 6.9 \times 10^{19}\ \mathrm{m^{-3}}$. The two latter species show a plateau only and an increase and the onset of a plateau, respectively. PSL2 was first measured as provided in $10^{-3}n$ KCl. Open squares on the other hand, denote the values obtained after a subsequent fast deionization. The increase of μ_{red} with decreased c is equivalent to the decrease with increased c observed for PS115. While the data set is still too small to reveal

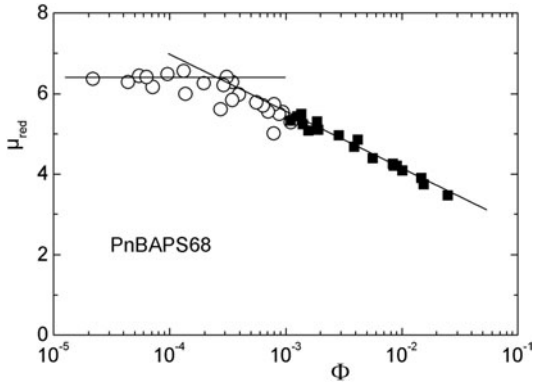

Figure 6. Reduced mobility μ_{red} versus packing fraction Φ for PnBAPS68 obtained using super heterodyne LDV. Symbols denote different structures: ○: isotropic fluid; ■: body centred cubic crystals. Lines are guides to the eye.

systematic correlations to particle size or surface group pK, we made an interesting observation for PSL2 for longer contact times with ion exchange resin. This sample showed decreasing μ_{red} with longer deionization times. Final values were observed to be of the order of 1.5–2. Further measurements on charge variable particles using super-heterodyne LDV are presently under way.

Using the new super heterodyne technique we investigated a further species of high charge and small diameter: PnBAPS68 [16, 21–24]. This species is characterized by its very small polydispersity and its comparable large charge, both leading to a low lying freezing transition. Further the scattering cross section is very small and samples stay transparent up to large packing fractions. The results are shown in figure 6. At low Φ the increase eludes detection similar to PSPSS3. On the other hand, we here for the first time were able to follow μ_{red} far into the crystalline phase, and even more importantly, observe a plateau of μ_{red} followed by a logarithmic decrease. Note that the end of the plateau and the freezing transition do not coincide and that the data run smoothly through the phase transition. Preliminary measurements on a second sample of same chemistry but slightly larger size confirm this trend [16].

4. Discussion

Low mobilities of isolated particles and the increase with Φ have been observed in some studies before [5, 11, 9, 33]. The reason for this behaviour remains unclear, with suggestions ranging from conduction behind the shear plane, over reduction of relaxation effects upon double layer overlap, to some kind of retardation effect exerted by neighbouring particles. In the plateau regime the mobility is large. Consistent with previous work by Deggelmann *et al* [6] this region may be entered also by decreasing the salt concentration at elevated packing fraction. The decrease of mobilities at higher particle concentrations was previously observed for interacting particles in an ordered state only for rod-like TMV-virus particles [7]. There it was attributed to a change of the state of dissociation of carboxyl virus surface groups. This possibility does not apply here, as our particles are stabilized by strong sulfate surface groups. For disordered or isolated particles, a decrease of μ is expected with increasing salt concentration at constant surface charge and also observed experimentally at large c [1, 2]. Here we increase the total ionic strength *via* the addition of further particles carrying additional counter-ions.

An interesting final point is that the mobility is not affected by the phase transition to the crystalline state occurring at about 6 μm^{-3}. This has been supported by additional measurements close to the phase transition, where the suspension is originally in the crystalline state but is shear molten in the course of time. In addition, there we found μ to be independent of the suspension structure. Previous studies had reported one or two data points for crystal mobilities similar to those of the fluid state [6, 9]. In both cases statistical arguments did not allow further interpretations. From conductance measurements, however, it is known that the conductivity is also not influenced by this phase transition [34, 35].

5. Conclusions

We have conducted measurements on several samples differing in particle size, surface group number and kind and under different salt concentrations. While for technical reasons it was not possible to cover more than four order of magnitude in particle concentration for an individual species, we have nevertheless observed reproducible trends for $\mu(\Phi)$. We therefore propose the existence of a universal shape of the $\mu(\Phi)$ curve: μ increases roughly logarithmically from low values for isolated particles to a plateau at rather large values. The plateau is followed by an approximately logarithmic decrease.

We have shown that the plateau value is different for different species. It decreases with increasing c. The location of the plateau region shifts to larger Φ with increased c. Transition 1, the start of the plateau, occurs once the contribution of the counter-ions starts dominating the salt concentration. Here the counter-ion contribution was calculated via $n_{\mathrm{Cl}} = nZ^*$, where Z^* is the effective charge from conductivity. It is observed in the region of parameters, where fluid order develops, which of course is defined only loosely as it is a rather gradual transition. No similarly simple correlation was observed for transition 2, the end of the plateau, neither in terms of ionic concentrations nor in terms of a correspondence to the freezing transition.

While the experimental determination of mobilities is now on solid ground, the interpretation of our data remains difficult. The existence of three different extended regions in the $\mu(\Phi)$ curves cannot be anticipated from previous experiments at elevated salt concentrations. There, pronounced maxima as a function of c were reported (often well explicable within the standard electrokinetic models [36]) but not as a function of particle concentration. Our observation of three distinct regions is also not immediately anticipated from a theoretical point of view, since the relations connecting μ to the surface or ζ-potential and ζ to some particle charge are highly nonlinear and not even monotonous [2, 37, 38]. In addition, it is not fully clear which charge one should refer to. Conventionally the number of dissociated surface groups Z is chosen. Alternatively it has been suggested that electrophoretic charges may relate to Alexander's (far field) effective charge Z^* [10, 28] which shows a saturation behaviour with increasing Z and can (in the absence of three body interactions [39]) be estimated from equilibrium properties like phase behaviour or elasticity. The latter is close but not identical to the conductivity charge derived under stationary non-equilibrium conditions [35]. Saturation behaviour on the other hand was also predicted for the effective surface potential [12]. Finally, it is not clear, whether the standard single particle electrokinetic theories mentioned above can be applied to ordering systems, or whether one has to assume conduction behind the plane of shear.

Certainly this Gemengelage of concepts, partially drawn from equilibrium, partly from non-equilibrium physics, calls for theoretical activity in close collaboration with simulation and experiment. We are, however, beginning to derive a coherent picture relating equilibrium and non-equilibrium properties of charged colloidal suspensions in a way that allows the prediction

of either from measurements or calculations of the other. We hope to have delivered a valuable and stimulating data base for further intense discussion of these issues.

Acknowledgments

It is a pleasure to thank Chr Holm, H Löwen, R Netz, C Mantegazza and H H v Grünberg for stimulating and sometimes intense discussions. We are grateful to the group of M Ballauff and the BASF for the kind supply of particles. Financial support of the Sonderforschungsbereich TR6-TPB1 is gratefully acknowledged. The work was further supported by the Deutsche Forschungsgemeinschaft (Grants Pa459/10, Pa459/11, SFB 625) and the Materialwissenschaftliches Forschungszentrum (MWFZ) Mainz.

References

[1] Hunter R J 1981 *Zeta-Potential in Colloidal Science* (London: Academic)
[2] Lyklema J 1993–2000 *Fundamentals of Interface and Colloid Science* vol 1–3 (London: Academic)
[3] Levin Y 2002 *Rep. Prog. Phys.* **65** 1577
[4] Sood A K 1991 *Solid State Phys.* **45** 1
[5] Okubo T 1987 *Ber. Bunsenges. Phys. Chem.* **91** 1064
[6] Deggelmann M, Palberg T, Hagenbüchle M, Maier E E, Krause R, Graf C and Weber R 1991 *J. Colloid Interface Sci.* **143** 318
[7] Deggelmann M, Graf C, Hagenbüchle M, Hoss U, Johner C, Kramer H G, Martin C and Weber R 1994 *J. Phys. Chem.* **98** 364
[8] Hidalgo-Alvarez R, Martin A, Fernandez A, Bastos D and de las Nieves F J 1996 *Adv. Colloid Interface Sci.* **67** 1
[9] Evers M, Garbow N, Hessinger D and Palberg T 1998 *Phys. Rev.* E **57** 6774
[10] de las Nieves F J, Barbero A F and Álvarez R H 1999 *Polymer Interfaces and Emulsions* ed K Esumi (New York: Dekker) chapter 5, pp 167–217
Fernandez-Nieves A, Fernandez-Barbero A and de las Nieves F J 2000 *Langmuir* **16** 4090
Pérez M Q, Fernández J C and Álvarez R H 2001 *J. Colloid Interface Sci.* **233** 280
[11] Garbow N, Evers M and Palberg T 2001 *Colloids Surf.* A **195** 227–41
[12] Ohshima H 2002 *J. Colloid Interface Sci.* **247** 18
Ohshima H 2003 *Colloid Surf.* A **222** 207
[13] Wette P, Schöpe H-J, Biehl R and Palberg T 2001 *J. Chem. Phys.* **114** 7556
[14] Schätzel K, Neumann W-G, Müller J and Materzok B 1992 *Appl. Opt.* **31** 770
[15] Garbow N, Müller J, Schätzel K and Palberg T 1997 *Physica* A **235** 291–305
[16] Medebach M 2004 Electrokinetics of low salt colloidal model suspensions *PhD Thesis* Mainz
Medebach M and Palberg T, unpublished
[17] Hunter R J 1981 *Zeta-Potential in Colloidal Science* (London: Academic)
[18] Komagata S 1933 *Res. Electrotech. Lab. Tokyo Commun.* **348** 1–114
[19] Palberg T, Mönch W, Schwarz J and Leiderer P 1995 *J. Chem. Phys.* **102** 5082–7
[20] Tsuchida A, Kuzawa M and Okubo T 2002 *Colloid Surf.* A **209** 235
[21] Medebach M and Palberg T 2004 *Prog. Colloid Polym. Sci.* **123** 260–3
[22] Medebach M and Palberg T 2003 *Colloid Surf.* A **222** 175–83
[23] Medebach M and Palberg T 2003 *J. Chem. Phys.* **119** 3360–70
[24] Medebach M and Palberg T 2004 Electrophoretic mobility of electrostatically interacting colloidal spheres *J. Phys.: Condens. Matter* at press
[25] Liu J, Schöpe H J and Palberg T 2000 *Part. Part. Syst. Charact.* **17** 206–12
Liu J, Schöpe H J and Palberg T 2000 *Part. Part. Syst. Charact.* **18** 50 (erratum)
[26] Hessinger D, Evers M and Palberg T 2000 *Phys. Rev.* E **61** 5493–506
[27] Uzgiris E E 1981 *Prog. Surf. Sci.* **10** 53
[28] Alexander S, Chaikin P M, Grant P, Morales G J, Pincus P and Hone D 1984 *J. Chem. Phys.* **80** 5776
[29] Groot R D 1991 *J. Chem. Phys.* **94** 5083
[30] Garbow N, Evers M, Palberg T and Okubo T 2004 On the electrophoretic mobility of isolated colloidal spheres *J. Phys.: Condens. Matter* **16** 3835–42

[31] Palberg T and Versmold H 1989 *J. Phys. Chem.* **93** 5296–310
[32] Okubo T 1987 *Ber. Bunsenges. Phys. Chem.* **91** 1064
[33] Bellini T, Degiorgio V, Mantegazza F, Marsan F A and Scarneccia C 1995 *J. Chem. Phys.* **103** 8228
[34] Hessinger D, Evers M and Palberg T 2000 *Phys. Rev.* E **61** 5493
[35] Wette P, Schöpe H J and Palberg T 2002 *J. Chem. Phys.* **116** 10981–8
[36] Antonietti M and Vorwerg L 1997 *Colloid Polym. Sci.* **275** 883
[37] O'Brien R W and White L R 1978 *J. Chem. Soc. Faraday Trans.* II **74** 1607
[38] Zukoski C F and Saville D A 1986 *J. Colloid Interface Sci.* **114** 32
Zukoski C F and Saville D A 1986 *J. Colloid Interface Sci.* **114** 45
[39] Hynninen A and Dijkstra M 2002 *Phys. Rev.* E **68** 021407